

# On the Efficiency of Various Deep Transfer Learning Models in Glitch Waveform Detection in Gravitational-Wave Data

Mesuga, Reymond<sup>1,\*</sup> and Bayanay, Brian James<sup>1</sup>

<sup>1</sup>*Department of Physical Sciences, Polytechnic University of the Philippines, Sta. Mesa, Manila*

\*Corresponding author: rmesuga@iskolarngbayan.pup.edu.ph

## Abstract

LIGO is considered the most sensitive and complicated gravitational experiment ever built. Its main objective is to detect the gravitational wave from the strongest events in the universe by observing if the length of its 4-kilometer arms change by a distance 10,000 times smaller than the diameter of a proton. Due to its sensitivity, LIGO is prone to the disturbance of external noises which affects the data being collected to detect the gravitational wave. These noises are commonly called by the LIGO community as glitches. The general objective of this study is to evaluate the efficiency of various deep transfer learning models namely VGG19, ResNet50V2, VGG16 and ResNet101 to detect glitch waveform in gravitational wave data. The accuracy achieved by the said models are 98.98%, 98.35%, 97.56% and 94.73% respectively. Even though the models achieved fairly high accuracy, it is observed that all of the model suffered from the lack of data for certain classes which is the main concern based on the results of the experiment.

Keywords: LIGO, gravitational wave, glitches, deep transfer learning model, VGG19, ResNet50V2, VGG16, ResNet101

## 1 Introduction

Gravitational waves (GWs) are deformations in spacetime that result from astrophysical phenomena involving celestial objects of masses much heavier than that of the sun moving at speeds up to a significant fraction of the speed of light, mainly called compact objects. GWs result from either mergers of binaries of compact objects, such as binary black hole (BBH) mergers, binary neutron star (BNS) mergers, neutron star-black hole binaries, white dwarf binaries, etc., or from self-production by a massive release of energy from astrophysical phenomena like stellar collapse (supernovae).

Ever since the first direct detection of GWs by the LIGO Collaboration on September 14, 2015, the field of gravitational-wave astronomy has become one of the rising fields of research in contemporary physics, and with upgrades to the LIGO detectors in the US as well the VIRGO detector in Italy, combined with the newly-operational KAGRA Observatory in Japan and the operation of the LISA Mission in future years, more and more GW events are being and will be detected, and with these detections come terabytes of data that are in great need of accurate analysis, to ensure that the signals that these observatories are indeed signals from outer space and not noise, either of terrestrial or electromagnetic origin. To build a somewhat good foundation of how the GW event data is being gathered, it is a must to give a short elaboration on the experimental setup of these observatories.

In the case of LIGO-Hanford and LIGO-Livingston, based in the United States, the 2 observatories are ground-based Michelson interferometers with arms spanning 4 km, where a 20-watt laser is fired, passing through a power recycling mirror, which then fully transmits light incident from the laser and reflects light from the other side increasing the power of the light field between the mirror and the subsequent beam splitter. From the beam splitter, the light travels along two orthogonal arms, and by using partially reflecting mirrors, Fabry–Pérot cavities are created in both arms that increase the effective path length of laser light in the arm. When a GW of sufficient energy passes through the interferometer, the spacetime in the local area is deformed, manifested through the effective change in length of one or both Fabry–Pérot cavities. This change in length will cause the light in the cavity to be slightly out of phase with the incoming light, which will lead to the cavity/s being out of coherence, and the laser light, which are tuned to destructively interfere at the detectors, will have a slightly periodically varying detuning, resulting in a measurable signal, with the detectors’ sensitivities up to lengths 10000 times smaller than the diameter of the proton [1]. Due to this and the LIGO-US detectors being ground-based, factors such as instrument noise and environmental influence [2] to name a few, the LIGO detectors not only records the GW strain data, but also over 200,000 *auxiliary channels* that monitor instrument behavior and environmental conditions [3]. Then, the GW strain data and the data from the auxiliary channels (which may or may not contain legitimate GW strain data) are then subject to data analysis.

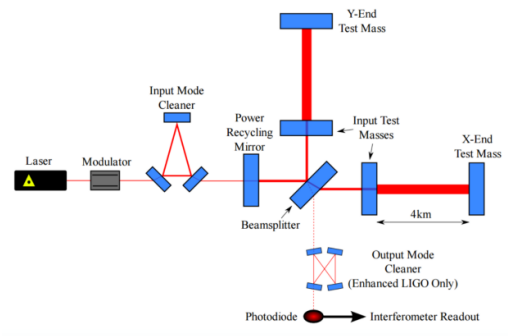


Fig. 1. Experimental setup of the Advanced LIGO Detector

In the analysis of GW data, of particular concern are transient, non-Gaussian noise features, called *glitches*, which are instrumental or environmental in nature (caused by e.g., small ground motions, ringing of the test-mass suspension system at resonant frequencies, or fluctuations in the laser) and come in a wide variety of time-frequency-amplitude morphologies [4], and can mimic true gravitational wave signals and can hinder sensitivity conditions [5]. These glitches are then classified by common origin and/or similar morphological characteristics [4].

The most used method used in the identification and classification of glitches in GW data is by means of **machine learning** algorithms [5, 6, 7, 8, 9, 10, 11] such as dictionary learning [5], similarity learning [6], deep transfer learning [7] among many a method. Building on this, the LIGO-Virgo Collaboration has advocated citizen science involvements in the search for these glitches, e.g., *Gravity Spy* [1], which speeds up the process of refining the increasingly large amount of GW data.

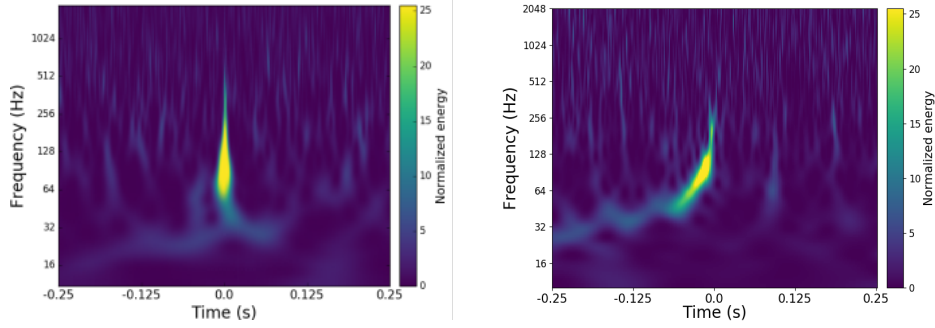


Fig. 2. Comparison of images from a glitch signal (left) and a GW signal (right) in LIGO O2 data

The refining of GW data is of paramount importance to the scientific community, particularly to physicists working in general relativity, cosmology, astrophysics, quantum gravity, etc. because the phenomenon itself serves as a validity of theories of gravity, mainly general relativity, and opens new questions to various fields in physics, like the mass threshold at which GW should occur, one of particular interest is the most recent detection (O3) of LIGO-Virgo, GW190814 [12], which indicates a “mass gap” between the heaviest neutron stars and the lightest black holes. These GW data is also used in the investigation of the Hubble expansion of the universe [13, 14], cosmic inflation via the existence of a stochastic gravitational-wave background [15, 16], existence of dark matter [17], among many new physics. With that being said, the efficiency of the different machine learning algorithms used in searching, classifying. and mitigating glitches should be considered, in order to obtain the most accurate data possible, and for this purpose, this experiment aims to compare some of the different machine learning algorithms used in noise detection in GW data, and their respective efficiencies in doing so.

The use of deep learning algorithms will be adopted in this paper. Deep learning (DL) is a type of machine learning algorithm (ML) where it uses a so called *artificial neural network* (ANN) to learn from different input data (i.e., images, sounds and texts) [18, 19]. ANN was inspired on how the human brain works. In fact, ANN has its own version of neuron that functions almost similar to biological neuron called *artificial neuron* which represents the nodes that can be found in the hidden layer (see Fig. 3). In a biological neuron, if the signals of information received by the synapse are strong enough (or surpass a certain threshold) [19]. When it comes to artificial neuron, if the weight of an input is not enough then the neuron will not be activated. In an image classification problem, each pixels on the image will serve as the inputs in input layer (see Fig. 3).

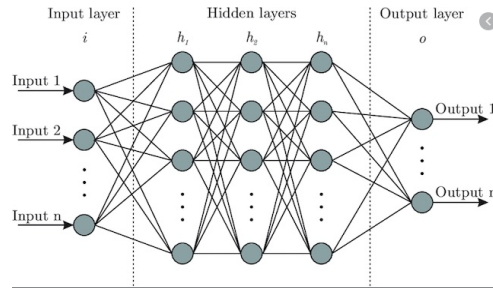


Fig. 3. A simple diagram of artificial neural network, [26]

After setting the pixels of an image as inputs, the ANN will then apply a randomly selected weights and multiply each on inputs. This can be defined as:

$$y = w * x + b \quad (1)$$

where  $y$  is the output,  $w$  is the weight,  $x$  is the input and  $b$  is a special kind of weight called bias. This function is the equation of the line.

Unfortunately, ANN (or/and DL algorithms in general) won't give any meaningful results just by just using a linear transformation. The application of non-linearity is needed because inputs such as images, sounds and texts are naturally non-linear. To apply non-linearity, each neuron on the hidden layer needs a so called *activation function*. Now, the output  $y$  on each neuron can be defined as:

$$y = \varphi(x * w + b) \quad (2)$$

where  $\varphi$  is the activation function. Note that equation 2 only represents an output  $y$  using a single input  $x$ . In general, output  $y$  of a neuron is the summation of all input  $x$  with their corresponding weights and bias and can be defined as equation (3):

$$y_k = \varphi\left(\sum_{i=0}^m x_i * w_{ki} + b_k\right) \quad (3)$$

$$\sum_{i=0}^m x_i * w_{ki} + b_k \quad (4)$$

The most common and up-to-date activation function is the ReLU activation function. This can be defined as:

$$f(x) = \max(0, x) \quad (5)$$

The idea here is that, if the value of equation (4) is less than or equal to zero, the output  $y$  will be automatically set as zero and will be deactivated, Otherwise, if it is greater than zero, then the output  $y$  will stay as it is and hence activated [20].

Now, someone cannot expect a deep learning model to have an accurate and meaningful result just by using a random selected weights. In order for a deep learning model to have a more accurate result, the model need to be trained. Training the model involves the adjustments of the weights. These weights need to be adjusted in a way that it fits on what is needed by the model to give more accurate result. These adjustments will continue as long as the model has not reached yet its minimum loss. The measurement of loss will be done using a *Loss Function* which measures how good or bad a deep learning is to classify each classes on the dataset. The most common and up-to-date loss function used in a multi-class image classification is the *Categorical Cross Entropy Loss* [22]. Meanwhile, the most common and up-to-date optimization algorithm that is used to adjust the weights is called the *Adam*

*Optimizer* [21]. This is the simple approach to understand how artificial neural network (ANN) works in an image classification.

That is, by setting the the pixels of an image as an inputs, applying random weights on each inputs, applying non-linear transformation on each inputs with their corresponding weights using activation function, training the model to lower the loss measured by a loss function and adjusting the weights using the optimizer.

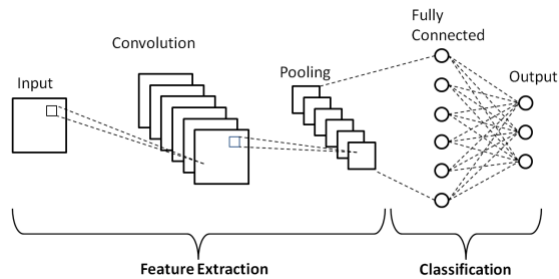


Fig. 4. Basic structure of Convolutional Neural Network (CNN), [23]

Artificial neural network (ANN) has many variations of algorithms. The most successful ANN algorithm is called Convolutional Neural Network (also called as CNN or ConvNet) [23, 24]. The structure of CNN can be divided into two parts which are the base and the head. The base of CNN is used to extract the features from an image and is formed primarily of three basic layers namely *convolution layer*, *ReLU activation layer* and *maximum pooling layer*. On the other hand, the head of the CNN is responsible for determining the class of the image. The main usage of convolution layer is to filter an image for a particular feature. Meanwhile, ReLU activation detects the feature within the filtered image and maximum pooling is responsible for the enhancement [24].

The general objective of the study is to evaluate the efficiency of various deep transfer learning models in glitch waveform detection in gravitational-wave data. The specific objectives are as follows: a) Identify what model has the highest and lowest accuracy in glitch waveform detection in gravitational-wave data and b) How does the quantity of the classes in the dataset affect the performance of the models.

## 2. Methodology

### 2.1 Data Set Preparation

The dataset used in this study will be gathered from a Kaggle repository that has been classified as a part of the Gravitational Spy Zooniverse [1]. The only difference between the Kaggle and original version of dataset is that images found in a Kaggle repository have no axes and were divided into training set, validation set and test set.

Table 1: Classes and their corresponding no. of images

Class	No. of Images	Class	No. of Images
Blip	1821	Whistle	299
Koi_Fish	706	Helix	279
Low_Frequency_Burst	621	Repeating_Blips	263
Light_Modulation	512	No_Glitch	150

Power_Line	449	Tomte	103
Extremely_Loud	447	1400Ripples	81
Low_Frequency_Lines	447	None_of_the_Above	81
Scattered_Light	443	Chirp	60
Violin_Mode	412	Air_Compressor	58
Scratchy	337	Wandering_Line	42
1080Lines	328	Paired_Doves	27

Table 1 shows the number of images for each class found in the dataset. As observed, the class Blip contains the majority of images which has 1821 images and the classes 1400Ripples, None\_of\_the\_Above, Chirp, Air\_Compressor, Wandering\_Line and Paired\_Doves did not even make it above a hundred. As mentioned earlier, the dataset was already divided into three sub-folders namely training set, validation set and test set. The training set contains 22348 images, the validation set contains 4800 images and test set contains 4720 images. It is important for a training set to have the majority of the images because it is the portion of the dataset that will be used during training.

## 2.2 Deep Transfer Learning Models

The type of deepl learning models that will be used in the experiment are all deep transfer learning model. Deep transfer learning or simply transfer learning uses pre-trained architectures as its base model. As mentioned in section I, the structure or architecture of convolutional neural network (CNN) can be divided into two parts (i.e., base and head). Most transfer learning model uses CNN architecture as well. The only difference is that, the base of transfer learning models were trained already using different images in the past. The most notable dataset that is commonly used to train a base for a pre-trained model is called ImageNet which contains 1.2 million images that has 1000 different classes [25]. The following pre-trained architectures that will be used as a base are as follows: ResNet101 [26], ResNet50V2 [27], VGG16 [28], and VGG19 [28]. The head of the models that will be used in the experiment can be visualize in Fig. 5.

Table 2: Summary of the model

Division	Layer (type)	Output Shape	No. of Parameters
Base	Pre-trained Base Architecture (Functional)	(None, 8, 8, 2048)	No. of Base Parameters
Head	Dropout	(None, 8, 8, 2048)	0
	Batch Normalization	(None, 8, 8, 2048)	8192
	Flatten	(None, 131072)	0
	Dense	(None, 512)	67109376
	Dense	(None, 22)	11286

Table 2 shows the summary of the model. Note that, Pre-trained Base Architecture will vary depending on what is used at the moment. The No. of Base Parameter will also vary depending on the

base. The head of the deep transfer learning models contains the layers as follows: Dropout, Batch Normalization, Flatten and two final Dense layers. The last Dense layer, as you can see on Table 1, has 22 output. That is because the dataset being used contains 22 classes. The metrics that will be used to compare the performance of the models are as follows: Test Accuracy, Precision, recall, f1-score and support.

### 3 Results and Discussion

This section is dedicated only data visualization and discussion of the results of the transfer learning models with following base architecture: ResNet101, ResNet50V2, VGG16, and VGG19.

#### 3.1 Results for ResNet101

Table 3: Metric Results of the model with ResNet101 base

Model Accuracy on Test Data:94.72620487213135%

	precision	recall	f1-score	support
Blip	0.60	0.97	0.74	1092
Koi Fish	0.72	0.83	0.77	408
Low Frequency Burst	0.58	0.82	0.68	360
Light Modulation	0.74	0.82	0.78	312
Power Line	0.80	0.99	0.88	272
Extremely Loud	1.00	0.11	0.20	256
Low Frequency Lines	0.83	0.73	0.78	264
Scattered Light	0.96	0.88	0.92	268
Violin Mode	0.79	0.04	0.08	256
Scratchy	1.00	0.01	0.01	200
1080Lines	0.39	0.81	0.53	200
Whistle	0.35	0.31	0.33	180
Helix	0.16	0.05	0.08	168
Repeating Blips	1.00	0.16	0.27	148
No Glitch	0.00	0.00	0.00	84
Tomte	0.37	0.77	0.50	52
1400Ripples	0.00	0.00	0.00	36
None of the Above	0.00	0.00	0.00	44
Chirp	0.50	0.03	0.05	40
Air Compressor	0.17	0.06	0.08	36
Wandering Line	0.00	0.00	0.00	28
Paired Doves	0.00	0.00	0.00	16

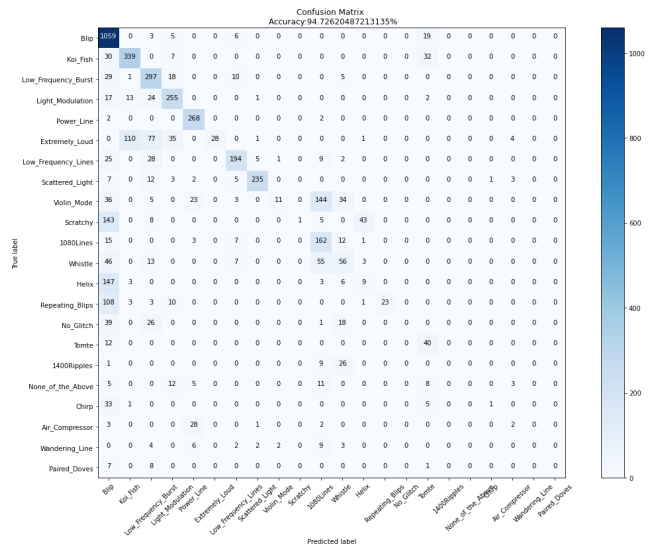


Fig. 5: Confusion matrix of the model with ResNet101 base

The results on Table 3 shows the metric results for the model with ResNet50 base. The metric results includes precision, recall, f1-score and support. The precision on Table 3 refers to the ability of a model not to label an instance positive that is actually negative. For each class, it is defined as the ratio of true positives to the sum of a true positive and false positive. In the case of the model with ResNet101 base, the classes that has the highest precision are Extremely Loud, Scratchy and Repeating Blips. This result is pretty surprising because the when you look at the confusion matrix in Fig. 5, the model did not predicted any false positives. But higher precision does not mean that the model predicted those classes perfectly. For instance, for class Extremely Loud, confusion matrix shows that the model detected 28 images for true positives while the remaining 419 images were falsely detected by other classes. Recall is the ability of a classifier to find all positive instances. It can be defined as the fraction of true positives to the sum of true positives and false negative. The class that has the highest recall is Blip. This result is not surprising because the class Blip also has the highest quantity of images so it

has a higher probability to find more positive instances than the remaining classes. F1-score is a weighted harmonic mean of precision and recall where the best score is 1.0 and the worst is 0.0. Using F1-score is good for comparing different models predicting the same thing. In the case of the model above, the class that has the highest F1-score is the Scattered Light. This result is somewhat surprising because the class that has the highest quantity of images commonly has the highest score. The model performed poorly to classify the fourteen classes mostly due to lack of quantity.

### 3.2 Results for VGG19

Table 4: Metric Results of the model with VGG19 base

Model Accuracy on Test Data:98.98101091384888%

	precision	recall	f1-score	support
Blip	0.94	0.98	0.96	1092
Koi_Fish	0.86	0.99	0.92	408
Low_Frequency_Burst	0.78	0.92	0.85	360
Light_Modulation	0.98	0.77	0.86	312
Power_Line	0.92	0.99	0.96	272
Low_Frequency_Lines	0.88	0.75	0.81	264
Extremely_Loud	0.93	0.91	0.92	256
Scattered_Light	0.98	0.91	0.94	268
Violin_Mode	0.87	0.88	0.88	256
Scratchy	0.95	0.98	0.97	200
1080Lines	0.63	0.94	0.76	200
Whistle	0.99	0.87	0.93	180
Helix	1.00	0.91	0.95	168
Repeating_Blips	0.93	0.77	0.84	148
No_Glitch	0.25	0.01	0.02	84
Tomte	0.76	0.81	0.79	52
1400Ripples	0.67	0.89	0.76	36
None_of_the_Above	0.57	0.57	0.57	44
Chirp	1.00	0.82	0.90	40
Air_Compressor	0.97	0.81	0.88	36
Wandering_Line	0.83	0.71	0.77	28
Paired_Doves	0.00	0.00	0.00	16

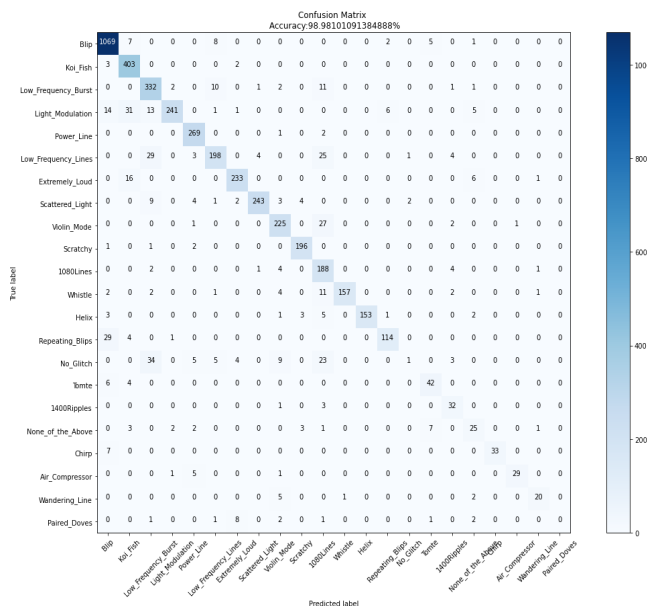


Fig. 6: Confusion matrix of the model with VGG19 base

Table 4 shows the metric results for the model with VGG19 base while Figure 6 shows its confusion matrix. The class Scratchy received the highest f1-score of 0.97 followed by Blip and Power\_Line with 0.96. If a score is a good indicator how good or bad the model is when classifying images from each set. The only class that it failed to classify is Paired\_Doves with f1-score of 0.0. This is not surprising at all because as observe in the previous model (i.e., ResNet101), the model is expected to perform poorly on the class with significantly lower quantity of images with respect to other classes. As observed in the confusion matrix of the model shown in Figure 6, the diagonal line is very visible as it performed better to classify the latter half of the classes that ResNet101. One of its downside is that its performance is substancial for classes with lower quantities of images. Another is that it performs poorly to classify images without glitches as it ightly classify only 1 out of 150 images. The final accuracy of the model is 98.98 percent which was achieved mainly using the classes with significantly higher quantity of images as it performed better when it comes to the first half of the classes.



### 3.3 Results for ResNet50V2

Table 5: Metric Results of the model with ResNet50V2 base

Model Accuracy on Test Data:98.35050106048584%

	precision	recall	f1-score	support
Blip	0.95	0.93	0.94	1092
Koi_Fish	0.82	0.96	0.89	408
Low_Frequency_Burst	0.86	0.90	0.88	360
Light_Modulation	0.90	0.87	0.88	312
Power_Line	0.97	0.86	0.91	272
Low_Frequency_Lines	0.78	0.64	0.70	264
Extremely_Loud	0.88	0.97	0.92	256
Scattered_Light	1.00	0.80	0.89	268
Violin_Mode	0.87	0.88	0.87	256
Scratchy	0.92	0.94	0.93	200
1080Lines	0.51	0.94	0.66	200
Whistle	0.84	0.87	0.85	180
Helix	0.93	0.99	0.96	168
Repeating_Blips	0.85	0.78	0.81	148
No_Glitch	0.58	0.21	0.31	84
Tomte	0.75	0.85	0.79	52
None_of_the_Above	0.61	0.39	0.47	44
1400Ripples	0.38	0.14	0.20	36
Chirp	0.83	0.60	0.70	40
Air_Compressor	0.89	0.67	0.76	36
Wandering_Line	0.81	0.75	0.78	28
Paired_Doves	1.00	0.44	0.61	16

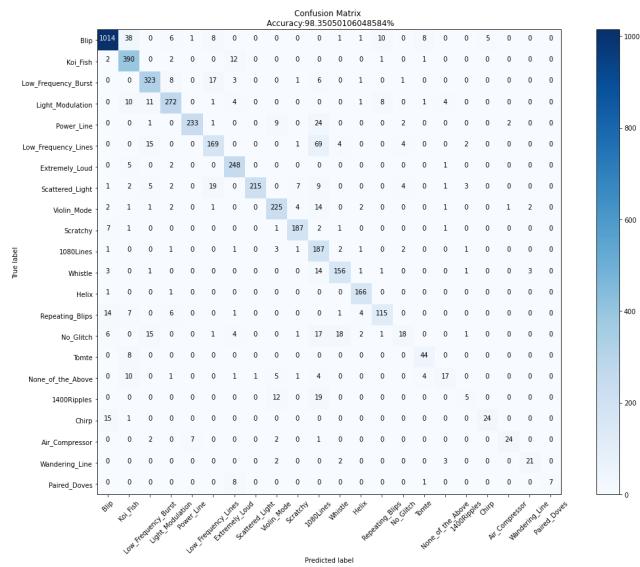


Fig. 7: Confusion matrix of the model with ResNet50V2 base

Table 5 shows the metric results for the mode with ResNet50 base while Figure 7 shows its confusion matrix. The model achieved 98.35 accuracy which is higher than that of ResNet101 and slightly lower than that of VGG19. The class Helix achieved the highest f1-score of 0.96 which means that it is the class where the model performed the best. The first half the the classes also have a decent f1-scores due to the fact that most of these classes contains a significantly higher quantity of images resulting to better performance. Meanwhile, the latter classes that contains fewer images has lower f1-score which is expected as observed from the results of previous models. The class Helix is an exception here because even though it only contains 279 images which is fewer than the majority that of first half classes, it still achieved the highest f1-score. Another interesting insights from the results for this model is that it has no 0 value of f1-score which means that the model is capable of classifying more than zero quantity of the image for each classes. In the case of VGG19, the class 1400Ripples contains the least quantity of rightly classified images which is only 5 images. Even though it achieved lower accuracy than that of VGG19, this model still able to classify at least 5 images and no more less.

### 3.4 Results for VGG16

Table 6: Metric Results of the model with VGG16 base

Model Accuracy on Test Data:97.56414294242859%

	precision	recall	f1-score	support
Blip	0.82	0.98	0.89	1092
Koi_Fish	0.87	0.90	0.89	408
Low_Frequency_Burst	0.87	0.69	0.77	360
Light_Modulation	0.80	0.75	0.77	312
Power_Line	0.92	0.65	0.77	272
Extremely_Loud	0.85	0.91	0.88	256
Low_Frequency_Lines	0.62	0.91	0.74	264
Scattered_Light	1.00	0.84	0.91	268
Violin_Mode	0.92	0.52	0.67	256
Scratchy	0.90	0.91	0.91	200
1080Lines	0.94	0.68	0.79	200
Whistle	0.91	0.79	0.85	180
Helix	0.83	0.97	0.90	168
Repeating_Blips	0.78	0.77	0.77	148
No_Glitch	0.08	0.11	0.09	84
Tomte	0.89	0.33	0.48	52
None_of_the_Above	0.43	0.30	0.35	44
1400Ripples	0.21	0.97	0.34	36
Chirp	1.00	0.35	0.52	40
Air_Compressor	1.00	0.19	0.33	36
Wandering_Line	1.00	0.36	0.53	28
Paired_Doves	0.25	0.06	0.10	16

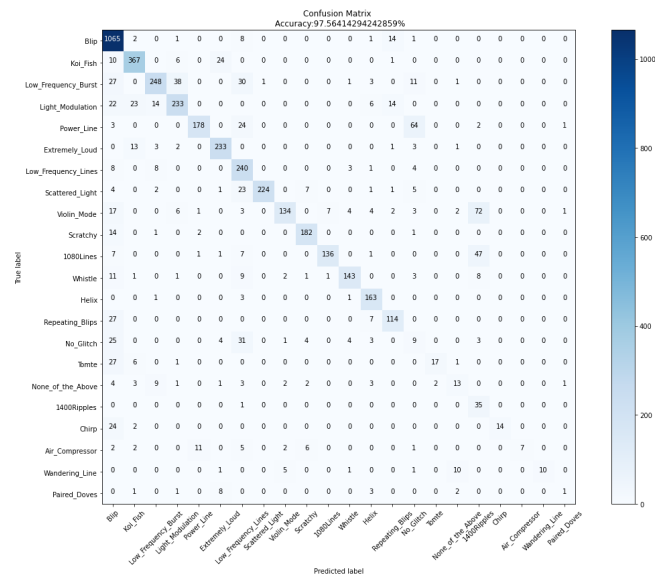


Fig. 8: Confusion matrix of the model with VGG16 base

Table 6 shows the metric results for VGG16 while Figure 8 shows its confusion matrix. The final accuracy of the model is 97.56 percent which is slightly lower than that of VGG19 and ResNet50V2 and slightly higher than that of ResNet101. The class Scratchy and Scattered\_Light achieved the highest f1-score with a value of 0.91 which means that the model did a good job at classifying these two classes. As expected, the first half of the classes will tend to have higher f1\_score compared to the second half because of limitation of the data. Another worth recognizing part of the result is the fact the the model also performed very well on the class Helix with the f1-score of 0.90. It is also observed that the model performed poorly to classify the class No\_Glitch with an f1-score of only 0.09. Another worth mentioning here is the fact that the model was able to classify at least more than zero images from all of the classes. The class called Paired\_Doves contains the least rightly classified image with the quantity of 1 out of 27 images.

## 4 Conclusion and Recommendations

The highest accuracy achieved by a deep learning involved in the study was 98.98% which was achieved by the model with VGG19 base. Meanwhile, the model with the base ResNet50V2, VGG16 and ResNet101 achieved 98.35%, 97.56% and 94.73% respectively. All of the model achieved a high accuracy although none of the model achieved to perfectly classify all the images in each classes. Another important insight worth mentioning here is the fact that many of the classes especially on the second half of the classes (see Table 1) contains a significantly fewer amount of data causing each of

the model to perform poorly on those classes. The high accuracies mentioned above tends to be bias on the classes with significantly higher amount of data due to the fact that the quantity of data really affect the performance of the model to classify each classes. This is the reason why each of the model tend to perform very well on some classes while perform poorly on other classes.

The authors of this paper would like to emphasize the importance of using significantly higher amount of data or images with more than 500 quantities as this number of images provides a descent performance for each model to classify better each of the classes. Another important information worth mentioning is the fact that some of the models tends to performed better to classify certain classes than the other. A good example is the result for the model with ResNet101 base where it is observed that the model really performed poorly on the second half of the classes to the point that it failed to rightly classify any of the images in many of the classes. Meanwhile, the rest of the model turns out to be able to classify those classes where the model with ResNet101 base tends to perform poorly. Although the f1-score of the said models is not considered high enough they are at least able to rightly classify more than or equal to 1 image from each class. These considerations may open up to the need of new deep learning algorithm dedicated only for detecting/classifying glitches. This is to classify better the glitches that interupts the gravitational wave detection.

## Acknowledgments

The authors of this paper would like thank Sir Mark Anthony Burgonio for allowing this study to be conducted under his supervision in the course Advance Laboratory 2.

## References

- [1] "Zooniverse," Zooniverse.org, 2021.  
<https://www.zooniverse.org/projects/zooniverse/gravity-spy/about/research> (accessed Jul. 04, 2021).
- [2] S. Doughton, "Ripples in space-time or 3-pound bird? Ravens at Hanford foul test of Einstein's theory," The Seattle Times, May 14, 2018.  
<https://www.seattletimes.com/seattle-news/science/suddenly-there-came-a-tapping-ravens-cause-blips-in-massive-physics-instrument-at-hanford/> (accessed Jul. 04, 2021).
- [3] B. P. Abbott et al., "Characterization of transient noise in Advanced LIGO relevant to gravitational wave signal GW150914," *Classical and Quantum Gravity*, vol. 33, no. 13, p. 134001, Jun. 2016, doi: 10.1088/0264-9381/33/13/134001.
- [4] M. Zevin, S. Coughlin, S. Bahaadini, E. Besler, N. Rohani, S. Allen, M. Cabero, K. Crowston, A. K. Katsaggelos, S. L. Larson, T. K. Lee, C. Lintott, T. B. Littenberg, A. Lundgren, C. Østerlund, J. R. Smith, L. Trouille, and V. Kalogera, "Gravity Spy: integrating advanced LIGO detector characterization, machine learning, and citizen science," *Classical and Quantum Gravity*, vol. 34, no. 6, p. 064003, 2017.

- [5] M. Llorens-Monteaagudo, A. Torres-Forné, J. A. Font, and A. Marquina, “Classification of gravitational-wave glitches via dictionary learning,” *Classical and Quantum Gravity*, vol. 36, no. 7, p. 075005, 2019.
- [6] S. Coughlin, S. Bahaadini, N. Rohani, M. Zevin, O. Patane, M. Harandi, C. Jackson, V. Noroozi, S. Allen, J. Areeda, M. Coughlin, P. Ruiz, C. P. L. Berry, K. Crowston, A. K. Katsaggelos, A. Lundgren, C. Østerlund, J. R. Smith, L. Trouille, and V. Kalogera, “Classifying the unknown: Discovering novel gravitational-wave detector glitches using similarity learning,” *Physical Review D*, vol. 99, no. 8, 2019.
- [7] George, Daniel, Shen, Hongyu, Huerta, E.A. (2017). *Glitch Classification and Clustering for LIGO with Deep Transfer Learning*. Workshop on Deep Learning for Physical Sciences (DLPS 2017), NIPS 2017, Long Beach, CA, USA.
- [8] R. E. Colgan, K. R. Corley, Y. Lau, I. Bartos, J. N. Wright, Z. Márka, and S. Márka, “Efficient gravitational-wave glitch identification from environmental data through machine learning,” *Physical Review D*, vol. 101, no. 10, 2020.
- [9] D. Davis, L. V. White, and P. R. Saulson, “Utilizing aLIGO glitch classifications to validate gravitational-wave candidates,” *Classical and Quantum Gravity*, vol. 37, no. 14, p. 145001, 2020.
- [10] S. Bahaadini, N. Rohani, S. Coughlin, M. Zevin, V. Kalogera, and A. K. Katsaggelos, “Deep multi-view models for glitch classification,” 2017 IEEE International Conference on Acoustics, Speech and Signal Processing (ICASSP), 2017.
- [11] S. Bahaadini et al., “Machine learning for Gravity Spy: Glitch classification and dataset,” *Information Sciences*, vol. 444, pp. 172–186, May 2018, doi: 10.1016/j.ins.2018.02.068.
- [12] R. Abbott et al., “GW190814: Gravitational Waves from the Coalescence of a 23 Solar Mass Black Hole with a 2.6 Solar Mass Compact Object,” *The Astrophysical Journal*, vol. 896, no. 2, p. L44, Jun. 2020, doi: 10.3847/2041-8213/ab960f.
- [13] J. Calderón Bustillo, S. Leong, T. Dietrich and P. Lasky, "Mapping the Universe Expansion: Enabling Percent-level Measurements of the Hubble Constant with a Single Binary Neutron-star Merger Detection", *The Astrophysical Journal Letters*, vol. 912, no. 1, p. L10, 2021. Available: 10.3847/2041-8213/abf502.
- [14] W. M. Farr, M. Fishbach, J. Ye, and D. E. Holz, “A Future Percent-level Measurement of the Hubble Expansion at Redshift 0.8 with Advanced LIGO,” *The Astrophysical Journal*, vol. 883, no. 2, p. L42, Oct. 2019, doi: 10.3847/2041-8213/ab4284.
- [15] “Gravitational waves from inflation,” *Www.sif.it*, 2015.  
<https://www.sif.it/riviste/sif/ncr/econtents/2016/039/09/article/0> (accessed Jul. 04, 2021).

- [16] R. H. Brandenberger, “Is the spectrum of gravitational waves the ‘Holy Grail’ of inflation?,” *The European Physical Journal C*, vol. 79, no. 5, May 2019, doi: 10.1140/epjc/s10052-019-6883-4.
- [17] Y. Michimura, T. Fujita, S. Morisaki, H. Nakatsuka, and I. Obata, “Ultralight vector dark matter search with auxiliary length channels of gravitational wave detectors,” *Physical Review D*, vol. 102, no. 10, Nov. 2020, doi: 10.1103/physrevd.102.102001.
- [18] A. U. Ruby, D. I. Prasannavenkatesan Theerthagiri, and Y. Vamsidhar, Binary cross entropy with deep learning technique for image classification, *International Journal* 9 (2020).
- [19] M. C. Nwadiugwu, “Neural Networks, Artificial Intelligence and the Computational Brain,” arXiv.org, 2020. <https://arxiv.org/abs/2101.08635> (accessed Jul. 04, 2021).
- [20] V. Nair and G. Hinton, “Rectified Linear Units Improve Restricted Boltzmann Machines,” [Online]. Available: <https://www.cs.toronto.edu/~fritz/absps/reluICML.pdf>.
- [21] I. Kandel, M. Castelli, and A. Popović, Comparative study of first order optimizers for image classification using convolutional neural networks on histopathology images, *Journal of Imaging* 6, 92 (2020).
- [22] A. U. Ruby, D. I. Prasannavenkatesan Theerthagiri, and Y. Vamsidhar, Binary cross entropy with deep learning technique for image classification, *International Journal* 9 (2020).
- [23] V. Phung and E. Rhee, A High-Accuracy Model Average Ensemble of Convolutional Neural Networks for Classification of Cloud Image Patches on Small Datasets, *Applied Sciences* 9 (2019)
- [24] A. Ghosh, Fundamental Concepts of Convolutional Neural Network, Recent Trends and Advances in Artificial Intelligence and Internet of Things, (2020)
- [25] A. Krizhevsky, ImageNet Classification with Deep Convolutional Neural Networks, *NeurIPS Proceedings*, (2012)
- [26] K. He, X. Zhang, S. Ren, and J. Sun, “Deep Residual Learning for Image Recognition,” Dec. 2015. [Online]. Available: <https://arxiv.org/pdf/1512.03385.pdf>.
- [27] K. He, X. Zhang, S. Ren, and J. Sun, “Identity Mappings in Deep Residual Networks,” arXiv.org, 2016. <https://arxiv.org/abs/1603.05027> (accessed Jul. 04, 2021).
- [28] K. Simonyan and A. Zisserman, “Published as a conference paper at ICLR 2015 VERY DEEP CONVOLUTIONAL NETWORKS FOR LARGE-SCALE IMAGE RECOGNITION,” 2015. [Online]. Available: <https://arxiv.org/pdf/1409.1556.pdf>.